organized brain regions, this limitation is less hampering, because the electrode conveys the activity of similarly tuned neurons (*21*, *22*). In contrast, because place cells in the hippocampus are distributed without topographic ordering (*23*), the LFP measured at any single location exhibits only weak place-modulation (fig. S9). However, compressed sensing methods can recover sparse signals even from mixed and subsampled measurements (*15*). During movement, population activity in the hippocampus is largely determined by a single (i.e., highly sparse) cause: the rat's current position. Therefore, distributed messages can be discovered by unsupervised learning methods such as ICA (*14*). Our experimental and simulation results show that the ICA-derived FFPs exhibit several properties reminiscent of place cells: They have smooth, localized place fields, exhibit phase precession, and show considerable trial-by-trial variability (*24*). Building on earlier work [e.g., (*25*)], these findings show how large-scale recordings of LFP can help in understanding the organization of activity in other brain regions, as well as developing robust decoders for brain-computer interfaces.

References and Notes

1. M. A. Wilson, B. L. McNaughton, *Science* **261**, 1055–1058 (1993).
2. W. J. Freeman, *Clin. Neurophysiol.* **115**, 2077–2088 (2004).
3. G. Buzsáki, C. A. Anastassiou, C. Koch, *Nat. Rev. Neurosci.* **13**, 407–420 (2012).
4. S. Łęski, H. Lindén, T. Tetzlaff, K. H. Pettersen, G. T. Einevoll, *PLOS Comput. Biol.* **9**, e1003137 (2013).
5. N. K. Logothetis, *J. Neurosci.* **23**, 3963–3971 (2003).
6. E. R. John, *Science* **177**, 850–864 (1972).
7. J. O'Keefe, L. Nadel, *The Hippocampus as a Cognitive Map* (Clarendon Press, Oxford Univ. Press, Oxford and New York, 1978).
8. C. H. Vanderwolf, *Electroencephalogr. Clin. Neurophysiol.* **26**, 407–418 (1969).
9. G. Buzsáki, E. I. Moser, *Nat. Neurosci.* **16**, 130–138 (2013).
10. C. Geisler *et al.*, *Proc. Natl. Acad. Sci. U.S.A.* **107**, 7957–7962 (2010).
11. A. Berényi *et al.*, *J. Neurophysiol.* **111**, 1132–1149 (2014).
12. O. Jensen, J. E. Lisman, *J. Neurophysiol.* **83**, 2602–2609 (2000).
13. K. Zhang, I. Ginzburg, B. L. McNaughton, T. J. Sejnowski, *J. Neurophysiol.* **79**, 1017–1044 (1998).
14. C. Hillar, F. T. Sommer, When can dictionary learning uniquely recover sparse data from subsamples? (2011); http://arxiv.org/abs/1106.3616).
15. D. L. Donoho, *Inf. Theory IEEE Trans. On* **52**, 1289–1306 (2006).
16. A. Hyvärinen, E. Oja, *Neural Netw.* **13**, 411–430 (2000).
17. M. Novey, T. Adali, *Proc. IEEE Workshop Mach. Learn. Signal Process* (Arlington, VA, 6 to 8 September, 2006), pp. 79–84.
18. A. Khosrowshahi *et al.*, *Exploring the Statistical Structure of Large-Scale Neural Recordings Using a Sparse Coding Model* (Cosyne, Salt Lake City, UT, 2010).
19. J. O'Keefe, M. L. Recce, *Hippocampus* **3**, 317–330 (1993).
20. E. Pastalkova, V. Itskov, A. Amarasingham, G. Buzsáki, *Science* **321**, 1322–1327 (2008).
21. C. Mehring *et al.*, *Nat. Neurosci.* **6**, 1253–1254 (2003).
22. A. de Cheveigné, J.-M. Edeline, Q. Gaucher, B. Gourévitch, *J. Neurophysiol.* **109**, 261–272 (2013).
23. A. D. Redish *et al.*, *J. Neurosci.* **21**, RC134 (2001).
24. R. Schmidt *et al.*, *J. Neurosci.* **29**, 13232–13241 (2009).
25. W. J. Freeman, B. Baird, *Behav. Neurosci.* **101**, 393–408 (1987).
26. K. Mizuseki, A. Sirota, E. Pastalkova, K. Diba, G. Buzsaki, Multiple single unit recordings from different rat hippocampal and entorhinal regions while the animals were performing multiple behavioral tasks (2013); available at http://crcns.org/data-sets/hc/hc-3.

Acknowledgments: This work was supported by NIH National Research Service Award fellowship no. 1F32MH093048 (G.A.); NSF CIF-D-018 no. 0937060 (I.H.S.); Marie Curie FP7-PEOPLE-2009-IOF grant no. 254780, EU-FP7-ERC-2013-Starting grant no. 337075, and the Lendület program of the Hungarian Academy of Sciences (A.B.); Japan Society for the Promotion of Science's Research Fellowship for Research Abroad (K.M.); NIH nos. NS-034994, MH-54671, and NS074015, NSF SBE no. 0542013, and the J. D. McDonnell Foundation (G.B.); NSF nos. 0855272 and 1219212 (F.S.). We thank D. Kaufman and J. Wolfe for advice on movies; C. Thanapirom for suggesting the Kuramoto model for rendering; K. D. Harris for suggestions about modeling; A. Khosrowshahi, J. Culpepper, C. Cadieu, and B. Olshausen for convolutional sparse coding; Walter Freeman for feedback; and members of the Buzsaki laboratory and the Redwood Center for discussions. All data collected from 32- to 64-electrode arrays is available in the hc-3 data set at crcns.org (*26*).

Supplementary Materials

www.sciencemag.org/content/344/6184/626/suppl/DC1
Materials and Methods
Figs. S1 to S10
Movies S1 and S2
References (*27*, *28*)

6 January 2014; accepted 14 April 2014
10.1126/science.1250444

Vascular and Neurogenic Rejuvenation of the Aging Mouse Brain by Young Systemic Factors

Lida Katsimpardi,[1,2]* Nadia K. Litterman,[1,2] Pamela A. Schein,[1,2] Christine M. Miller,[1,2,3] Francesco S. Loffredo,[1,2,4] Gregory R. Wojtkiewicz,[5] John W. Chen,[5] Richard T. Lee,[1,2,4] Amy J. Wagers,[1,2,3] Lee L. Rubin[1,2]*

In the adult central nervous system, the vasculature of the neurogenic niche regulates neural stem cell behavior by providing circulating and secreted factors. Age-related decline of neurogenesis and cognitive function is associated with reduced blood flow and decreased numbers of neural stem cells. Therefore, restoring the functionality of the niche should counteract some of the negative effects of aging. We show that factors found in young blood induce vascular remodeling, culminating in increased neurogenesis and improved olfactory discrimination in aging mice. Further, we show that GDF11 alone can improve the cerebral vasculature and enhance neurogenesis. The identification of factors that slow the age-dependent deterioration of the neurogenic niche in mice may constitute the basis for new methods of treating age-related neurodegenerative and neurovascular diseases.

In the adult brain, neural stem cells reside in a three-dimensional (3D) heterogeneous niche, where they are in direct contact with blood vessels and the cerebrospinal fluid. The vasculature can influence neural stem cell proliferation and differentiation by providing a local source of signaling molecules secreted from endothelial cells (*1*) as well as by delivering systemic regulatory factors (*2*). The hormone prolactin (*3*), dietary restriction (*4*), and an exercise/enriched environment (*5*) positively modulate neurogenesis, whereas increased levels of glucocorticoids associated with stress have the opposite effect (*6*). In the aging niche, the vasculature deteriorates with a consequent reduction in blood flow (*7*), and the neurogenic potential of neural stem cells declines, leading to reduced neuroplasticity and cognition (*8*–*10*). Systemic factors can also affect these aging-associated events, either positively in which circulating monocytes enhance remyelination in aged mice (*11*, *12*) or negatively in which the accumulation of chemokines in old blood can reduce neurogenesis and cognition in young mice (*10*).

To test whether the age-related decline of the neurogenic niche can be restored by extrinsic young signals, we used a mouse heterochronic parabiosis model. Our experiments reveal a remodeling of the aged cerebral vasculature in response to young systemic factors, producing noticeably greater blood flow, as well as activation of subventricular zone (SVZ) neural stem cell proliferation and enhanced olfactory neurogenesis, leading to an improvement in olfactory function. Furthermore, we tested GDF11, a circulating transforming growth factor–β (TGF-β) family member that reverses cardiac hypertrophy in aged mice (*13*), and found that it can also stimulate vascular remodeling and increase neurogenesis in aging mice. Thus, we have observed that age-dependent remodeling of this niche is reversible by means of systemic intervention.

[1]Department of Stem Cell and Regenerative Biology, Harvard University, Cambridge, MA 02138, USA. [2]Harvard Stem Cell Institute, Cambridge, MA 02138, USA. [3]Howard Hughes Medical Institute, Joslin Diabetes Center and the Paul F. Glenn Laboratories for the Biological Mechanisms of Aging, Harvard Medical School, Boston, MA 02115, USA. [4]Cardiovascular Division, Department of Medicine, Brigham and Women's Hospital, Boston, MA 02115, USA. [5]Center for Systems Biology and Department of Radiology, Massachusetts General Hospital, Harvard Medical School, Boston, MA 02115, USA.

*Corresponding author. E-mail: lee_rubin@harvard.edu (L.L.R.); lida_katsimpardi@harvard.edu (L.K.)

To test our hypothesis, we generated heterochronic parabiotic pairs between 15-month-old (Het-O) and 2-month-old (Het-Y) male mice, as well as control groups of age-matched pairs, namely isochronic young (Iso-Y) and isochronic old (Iso-O) pairs (fig. S1). The average lifespan of this strain of mice in the National Institute of Aging's growth conditions is 27 months. All parabiotic pairs remained surgically joined for 5 weeks (*14*). Because aging leads to a reduced number of progenitor cells (*15*–*17*), we assessed how heterochronic parabiosis can affect the SVZ neural stem cell populations by analyzing coronal SVZ sections (fig. S2A) of heterochronic and isochronic brains for different SVZ stem/progenitor cell types, such as proliferative Ki67$^+$ cells, Sox2$^+$ stem cells, and Olig2$^+$ transit amplifying progenitors (Fig. 1, A, B, and C, respectively). Quantification of these sections revealed an increase of 26.9% for Ki67$^+$ cells (fig. S2B), 112% for Sox2$^+$ cells (Fig. 1D), and 57% for Olig2$^+$ cells (Fig. 1E) in the Het-O compared with the Iso-O SVZ. However, these cell populations were unaffected in the Het-Y mice (Fig. 1, D and E, and fig.S2C). Systemic factors in old blood can have detrimental effects on hippocampal neurogenesis in young animals (*10*); however, we saw no decrease in neural stem/progenitor cell numbers in the SVZ of young mice joined to 15-month-old partners. We wondered whether this discrepancy was related to differences between the SVZ and the hippocampus or to the fact that our old animals were younger than the old animals used in the previous study. We therefore joined 2-month-old mice with 21-month-old mice (fig. S3A) and found that the older blood negatively affected young SVZ neurogenesis because Het-Y21 mice showed decreased proliferative Ki67$^+$ (fig. S3, B and D) and Sox2$^+$ cell populations (fig. S3, C and E) in the SVZ as compared with those of Iso-Y mice. These data are consistent with the previously reported negative effect of older blood on hippocampal neurogenesis (*10*) and indicate an age-dependent accumulation of factors in the blood of older mice that affect neurogenic zones in both the hippocampus and SVZ.

Aging results in longer cell-cycle times in precursor cells isolated from the SVZ (*18*). To assess the effect of heterochronic parabiosis on neural stem cell proliferation, we cultured neural stem cells from parabiotic brains as neurospheres (*19*, *20*). After the first passage, neurospheres derived from the Het-O SVZ were 43% larger in diameter than those derived from the Iso-O SVZ (fig. S4), and after removal of growth factors, they generated ~2.5-fold more TuJ1$^+$ neurons than did the Iso-O (fig. S5). This suggests that neural stem cells exposed to young systemic factors increase their ability to proliferate and differentiate into neurons. Collectively, these data demonstrate that youthful circulating factors can restore the self-renewal and differentiation potential of aged SVZ stem cells, and this effect can persist for some time after isolation from the mouse brain.

Adult SVZ neural stem and progenitor cells differentiate into neuroblasts and migrate through the rostral migratory stream to the olfactory bulb, where they mature into interneurons (*21*). We asked whether the increase in neural stem and progenitor cells could produce a subsequent change in olfactory neurogenesis in the Het-O mice. We pulsed parabiotic pairs with BrdU to label newborn neurons, and after 3 weeks, the mice were analyzed for BrdU$^+$/NeuN$^+$ cells to quantify newborn neurons (Fig. 2A). As expected from our in vitro studies, we observed increased olfactory neurogenesis in vivo. Het-O newborn neuron populations were enriched by 92% as compared with Iso-O populations (Fig. 2B). In accordance with our above results, the number of new neurons in Het-Y mice was only slightly negatively affected, although the decrease was not statistically significant (Fig. 2C).

To test the functional implication of these findings, we performed an olfaction assay in which naïve single parabionts, separated from their parabiotic partners after 5 weeks, were exposed to different concentrations of an odorant (*22*). After a short habituation period, each parabiont was presented with different concentrations of an odorant, and the total time that each parabiont spent exploring the odorant for each concentration was measured. In this assay, Het-O (Fig. 2D) and young control (Fig. 2D) mice both spent more time exploring a low concentration of odorant (diluted 10^5 times), whereas a high concentration (diluted 10 times) produced a negative response. In comparison, Iso-O mice spent roughly the same amount of time exploring the odorant regardless of its concentration (Fig. 2D). These results suggest that Het-O mice have a higher olfactory discrimination than do the Iso-O mice. Therefore, exposure of the neurogenic niche to young systemic factors enhances functional neurogenesis, culminating in improved olfactory behavior.

Cerebrovascular architecture, capillary density, and cerebral blood flow have been reported to decline with aging (*23*–*25*). Given the interconnection between the vasculature and neural stem cells, we asked whether young blood factors can also rejuvenate blood vessel architecture and function. To test this, we created "angiograms," 3D reconstructions of the blood vessels (fig. S6A). Volumetric analysis of these angiograms showed that aging causes a decrease in blood vessel volume, as expected (Fig. 3, A and B). However, heterochronic parabiosis reversed this decline, increasing blood vessel volume by 87% in the Het-O compared with the Iso-O group (Fig. 3, A and B). Furthermore, we

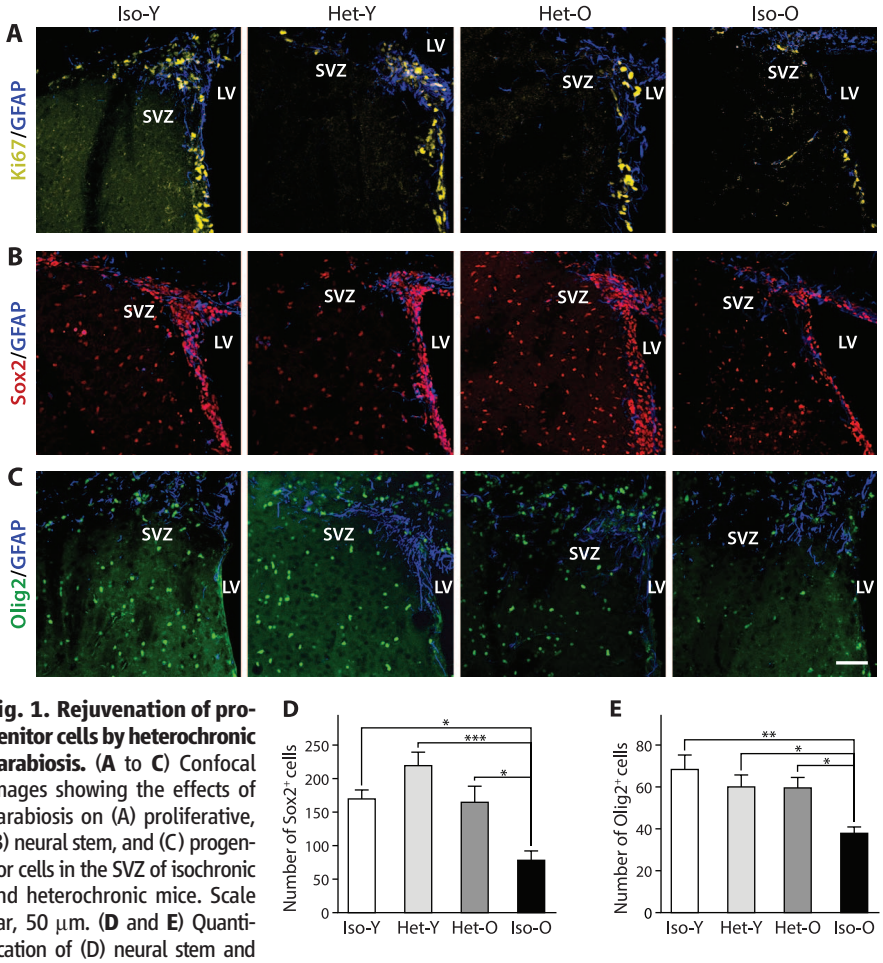

Fig. 1. Rejuvenation of progenitor cells by heterochronic parabiosis. (**A** to **C**) Confocal images showing the effects of parabiosis on (A) proliferative, (B) neural stem, and (C) progenitor cells in the SVZ of isochronic and heterochronic mice. Scale bar, 50 μm. (**D** and **E**) Quantification of (D) neural stem and (E) progenitor cell populations of the above images ($n = 9$ animals for each experimental group, $^*P < 0.05$, $^{**}P < 0.01$, $^{***}P < 0.001$). Data shown as mean ± SEM; statistical analysis was performed with analysis of variance (ANOVA).

observed that blood vessel branching increased by 21% in Het-O versus Iso-O mice (fig. S6B). Some blood vessels in the Het-O mice were not associated with AQP4$^+$ astrocytic endfeet, suggesting that these vessels are newly formed and potentially leaky, thus providing NSCs with enhanced nutritive support (fig. S6E). This phenomenon of vascular remodeling in the Het-O mice extended to other neurogenic areas such as the hippocampus (fig. S7, A and B) and also to non-neurogenic areas such as the cortex (Fig. S7C). To test whether the increased blood vessel volume led to functional improvement, we measured cerebral blood flow (CBF) with magnetic resonance imaging (MRI) in the parabiotic mice (Fig. 3E) because CBF is known to decrease with aging (*26*). We found that heterochronic parabiosis indeed restored CBF to the levels seen in young animals (Fig. 3, C, D, and E), indicating that the vascular remodeling observed in Het-O mice changes the hemodynamics of the vascular system in the central nervous system. Young vasculature, on the contrary, retained the same volumetric (Fig. 3, A and B), blood flow (fig. S6D), and branching (fig. S6C) characteristics in both isochronic and heterochronic parabiosis.

New vessels can form either by sprouting from existing capillaries or de novo from circulating

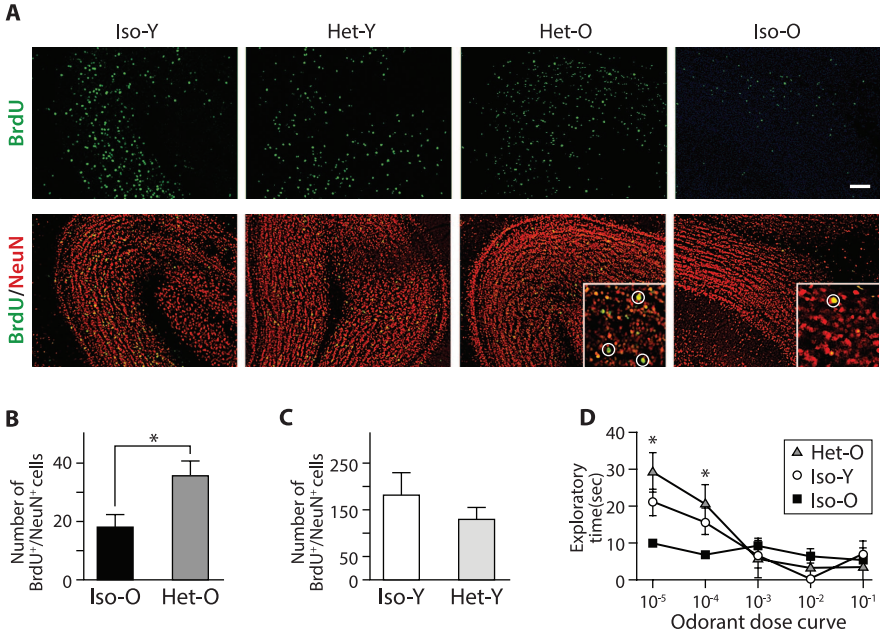

Fig. 2. Heterochronic parabiosis enhances neurogenesis and cognitive functions in the aging mouse. (**A**) Representative images of olfactory bulbs showing newborn neurons in isochronic and heterochronic parabionts. Scale bar, 100 μm. Circles in higher-magnification inserts indicate BrdU$^+$/NeuN$^+$ double-positive cells. (**B** and **C**) Quantification of neurogenesis in the olfactory bulbs of (B) old and (C) young parabionts (n = 4, *P < 0.05). (**D**) Measurement of the exploratory time during the olfactory sensitivity assay (n = 3). Data are shown as mean ± SEM; statistical analysis was performed with t test. "n" indicates the number of animals for each experimental group.

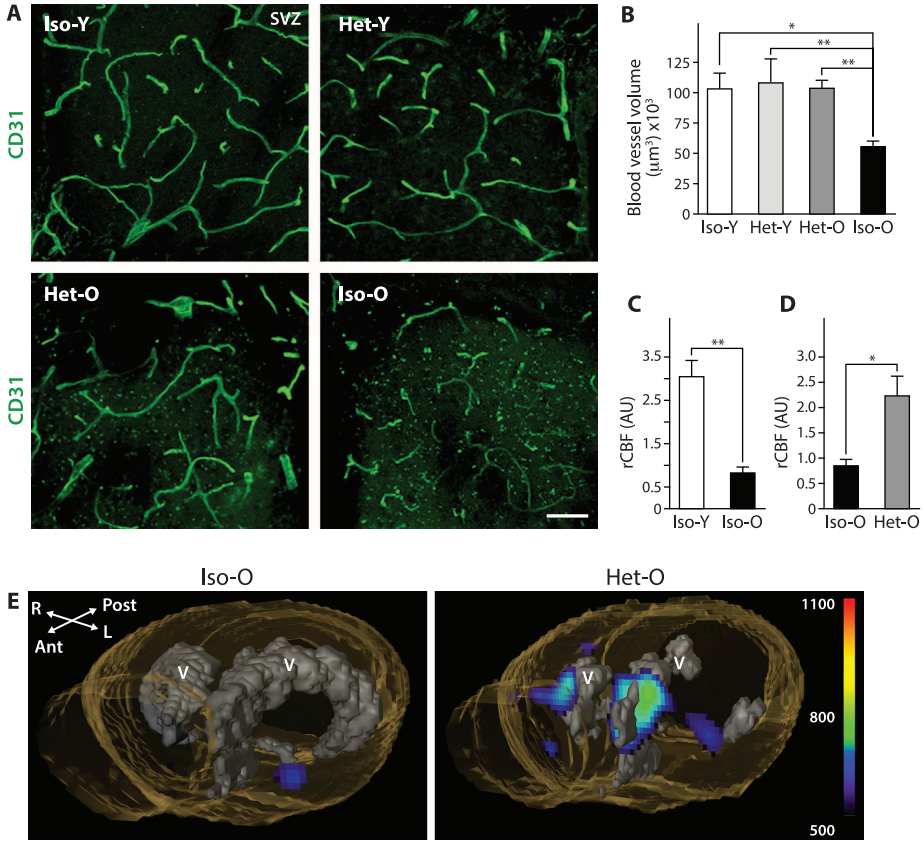

Fig. 3. Young blood induces vascular remodeling and increases blood flow in old mice. (**A**) Confocal images of the SVZ area showing the changes in vasculature after heterochronic parabiosis. Scale bar, 50 μm. (**B**) Measurement of blood vessel volume in isochronic and heterochronic parabionts (n_{old} = 9, n_{young} = 6). (**C** and **D**) Measurements of cerebral blood flow in the SVZ region of the parabionts: Iso-O versus (C) Iso-Y or (D) Het-O mice (n = 4). (**E**) Perfusion MRI images of the brain. "V" indicates the ventricles. Data are shown as mean ± SEM; statistical analysis was performed with ANOVA in (B) and t test in (C) and (D); *P < 0.05, **P < 0.01, ***P < 0.001. "n" indicates the number of animals for each experimental group.

endothelial progenitors. To test which of these mechanisms is taking place, we parabiotically joined young green fluorescent protein (GFP) mice with old non-GFP mice for 5 weeks. Analysis of these brains excluded any detectable contribution of young circulating endothelial progenitors to the vascular remodeling in Het-O animals (fig. S8). Because pericytes play a role in vasoconstriction in capillaries (*27*), we sought to investigate whether their numbers were altered by heterochronic parabiosis. The number of pericytes associated with blood vessels was unaffected by parabiosis (fig. S9). The likelihood that systemic factors can act directly on endothelial cells was further supported when we cultured primary mouse brain capillary endothelial cells and treated them with serum isolated from either young or old mice. Young serum stimulated endothelial cell proliferation by 88% as compared with old serum (fig. S10).

Several factors—including Sonic Hedgehog, erythropoietin, nitric oxide, Notch ligands, Fibroblast Growth Factor, and Vascular Endothelial Growth Factor (*28*–*31*)—that affect neurogenesis are also involved in blood vessel maintenance and proliferation. Of most relevance to our study are those factors that decrease with aging. Recently, one such factor—GDF11/BMP11, a circulating member of the BMP/TGF-β family—was found to be present in higher concentrations in young and heterochronic old than in old mouse serum. GDF11 administration to older mice reproduces many of the beneficial effects of parabiosis on aging hypertrophic cardiac muscle (*13*). This prompted us to test whether GDF11 could also restore the age-related decline in neurogenesis and participate in vascular remodeling. For that purpose, 21- to 23-month-old mice were treated with daily injections of either recombinant GDF11 (rGDF11, 0.1 mg/kg mouse body weight), a dosing regimen that increases GDF11 levels in old mice toward youthful levels (*13*), or phosphate-buffered saline (PBS) (vehicle) for 4 weeks, and their blood vessels were subsequently analyzed by using the volumetric assay described above. The volume of blood vessels in GDF11-treated old mice increased by 50% compared with the PBS-treated mice (Fig. 4, A and C). Moreover, the population of $Sox2^+$ cells in GDF11-treated old mice increased by 29% compared with the control (Fig. 4, B and D).

In vitro experiments confirmed that GDF11 acts, at least in part, on brain capillary endothelial cells. First, treating endothelial cells with rGDF11 (40 ng/ml) activates the well-known TGF-β signaling pathway in these cells, revealed by an increase in SMAD phosphorylation cascade (Fig. 4, E and F). Second, a 6-day treatment of primary brain capillary endothelial cells with rGDF11 (40 ng/ml) increased their proliferation by 22.9% as compared with that of controls (fig. S11), but not in the presence of a TGF-β inhibitor (fig. S12), confirming that GDF11 has a direct biological effect on these cells through the p-SMAD pathway.

The physiology of the brain is intimately dependent on its vasculature during aging. In the normal brain, there is a close association between stimulation of neural stem cells and blood vessels in the SVZ (*4*–*6*) and in the dentate gyrus. Here, we show that heterochronic parabiosis increases neurogenesis and improves vascularity and blood flow of the neurogenic niche. GDF11, a factor that also rejuvenates heart and skeletal muscle in aged mice (*32*), also was able to increase blood flow and neurogenesis in aged mice. Its effects were not as large as those of parabiosis itself, although that may relate to using suboptimal doses of this factor. In addition, some of its actions may be direct, and others may be indirect. Additional experiments will be needed to address this issue.

A question that arises from our work relates to aging-associated changes in the balance of positively and negatively acting circulating factors. We show here that blood from 15-month-old mice does not have a detrimental effect on young mice, whereas older blood (21 months old) dramatically decreases neural stem-cell populations in the young brain, an effect also observed in the hippocampus (*10*). This observation suggests that there is an age at which deleterious systemic factors accumulate and/or young factors are reduced. However, regardless of the age of the old brain, we and others (*10*, *11*) have shown that young blood is still able to rejuvenate the aged brain.

In conclusion, circulating factors, specifically including GDF11, have diverse positive effects in aging mice, including enhancing neurogenesis. Aging also affects the microvascular network in non-neurogenic regions of the brain (*7*). Circulating factors improved the vasculature in the cortex, as well as in other parts of the aging mouse brain. It is possible that increased blood flow might result in increased neural activity and function, opening new therapeutic strategies for treating age-related neurodegenerative conditions.

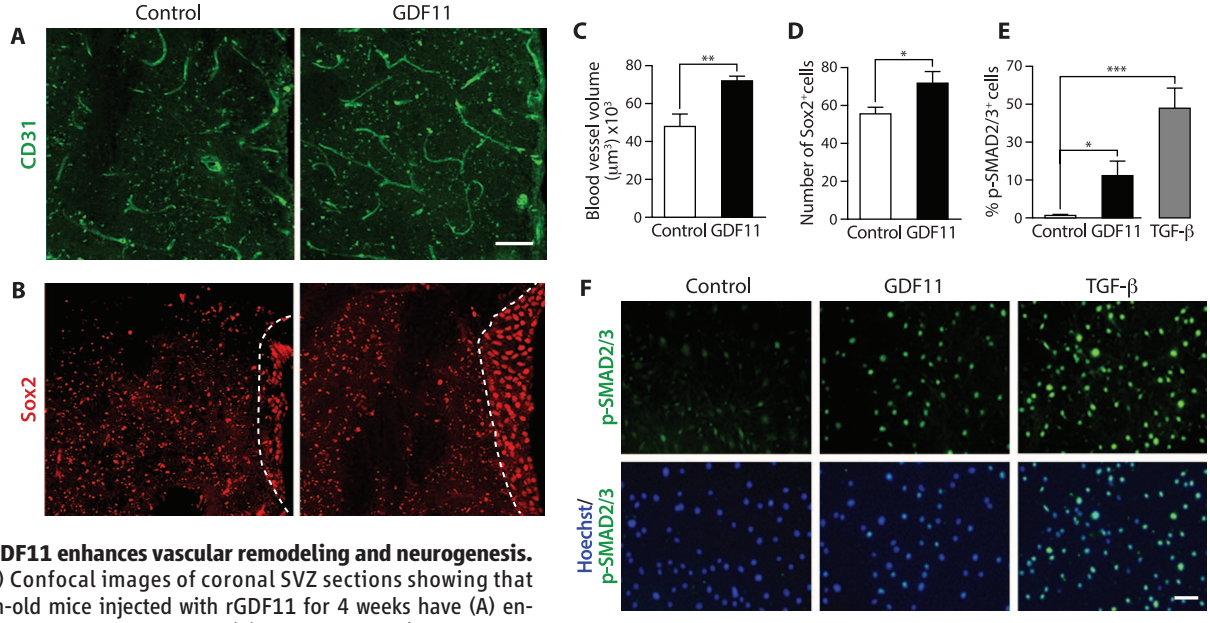

Fig. 4. GDF11 enhances vascular remodeling and neurogenesis. (**A** and **B**) Confocal images of coronal SVZ sections showing that 22-month-old mice injected with rGDF11 for 4 weeks have (A) enhanced vascularization as well as (B) increased $Sox2^+$ neural stem cell populations compared with those of control. (**C**) Measurement of blood vessel volume in rGDF11-treated and control mice ($n = 9$). (**D**) Quantification of $Sox2^+$ cells in the SVZ area ($n = 6$); "n" indicates the number of animals for each experimental group. (**E**) Quantification and (**F**) representative images of the percentage of phospho-$SMAD2/3^+$ cells in primary brain capillary endothelial cell cultures treated with either GDF11 (40ng/ml) or TFG-β (10ng/ml) in the presence of sodium orthovanadate used to inhibit phosphatase activity for 30 min ($n = 7$). Scale bar, 100 μm. Data are shown as mean ± SEM; statistical analysis was performed with t test, between each experimental condition and the untreated control; $^*P < 0.05$, $^{**}P < 0.01$, $^{***}P < 0.001$.

References and Notes

1. Q. Shen *et al.*, *Science* **304**, 1338–1340 (2004).
2. M. Tavazoie *et al.*, *Cell Stem Cell* **3**, 279–288 (2008).
3. T. Shingo *et al.*, *Science* **299**, 117–120 (2003).
4. P. Wu *et al.*, *Neurobiol. Aging* **29**, 1502–1511 (2008).
5. H. van Praag, G. Kempermann, F. H. Gage, *Nat. Neurosci.* **2**, 266–270 (1999).
6. J. S. Snyder, A. Soumier, M. Brewer, J. Pickel, H. A. Cameron, *Nature* **476**, 458 (2011).
7. E. Farkas, P. G. Luiten, *Prog. Neurobiol.* **64**, 575–611 (2001).
8. H. G. Kuhn, H. Dickinson-Anson, F. H. Gage, *J. Neurosci.* **16**, 2027–2033 (1996).
9. T. Seki, Y. Arai, *Neuroreport* **6**, 2479–2482 (1995).
10. S. A. Villeda *et al.*, *Nature* **477**, 90–94 (2011).
11. J. M. Ruckh *et al.*, *Cell Stem Cell* **10**, 96–103 (2012).
12. V. E. Miron *et al.*, *Nat. Neurosci.* **16**, 1211–1218 (2013).
13. F. S. Loffredo *et al.*, *Cell* **153**, 828–839 (2013).
14. D. E. Wright, A. J. Wagers, A. P. Gulati, F. L. Johnson, I. L. Weissman, *Science* **294**, 1933–1936 (2001).
15. T. Seki, *J. Neurosci. Res.* **70**, 327–334 (2002).
16. A. Garcia, B. Steiner, G. Kronenberg, A. Bick-Sander, G. Kempermann, *Aging Cell* **3**, 363–371 (2004).
17. J. Luo, S. B. Daniels, J. B. Lennington, R. Q. Notti, J. C. Conover, *Aging Cell* **5**, 139–152 (2006).
18. V. Tropepe, C. G. Craig, C. M. Morshead, D. van der Kooy, *J. Neurosci.* **17**, 7850–7859 (1997).
19. B. A. Reynolds, S. Weiss, *Science* **255**, 1707–1710 (1992).
20. L. Katsimpardi *et al.*, *Stem Cells* **26**, 1796–1807 (2008).
21. A. Carleton, L. T. Petreanu, R. Lansford, A. Alvarez-Buylla, P. M. Lledo, *Nat. Neurosci.* **6**, 507–518 (2003).
22. R. M. Witt, M. M. Galligan, J. R. Despinoy, R. Segal, *J. Vis. Exp.* **28**, 949 (2009).
23. M. J. Reed, J. M. Edelberg, *Sci. SAGE KE* **2004**, pe7 (2004).
24. A. Rivard *et al.*, *Circulation* **99**, 111–120 (1999).
25. D. R. Riddle, W. E. Sonntag, R. J. Lichtenwalner, *Ageing Res. Rev.* **2**, 149–168 (2003).
26. C. L. Grady *et al.*, *Neuroimage* **8**, 409–425 (1998).
27. R. Balabanov, P. Dore-Duffy, *J. Neurosci. Res.* **53**, 637–644 (1998).
28. P. Carmeliet, *Nat. Rev. Genet.* **4**, 710–720 (2003).
29. A. Alvarez-Buylla, D. A. Lim, *Neuron* **41**, 683–686 (2004).
30. M. Brines, A. Cerami, *Nat. Rev. Neurosci.* **6**, 484–494 (2005).
31. E. R. Matarredona, M. Murillo-Carretero, B. Moreno-López, C. Estrada, *Brain Res. Brain Res. Rev.* **49**, 355–366 (2005).
32. M. Sinha *et al.*, *Science* **344**, 649–652 (2014).

Acknowledgments: We thank C. McGillivray and D. Faria at the HSCRB Histology Core for providing help with sectioning and D. Smith and B. Götze at the HCBI for providing microscope facilities. We also thank W. Stallcup for providing the anti-NG2 antibody, C. Bonal for technical help and J. LaLonde for editorial assistance. This work was supported by a Senior Scholar in Aging Award from The Ellison Medical Foundation to L.L.R.; awards from GlaxoSmithKline and the Harvard Stem Cell Institute to L.L.R.; NIH (R01 AG032977 1R01 AG040019) to R.T.L.; and the Paul F. Glenn Foundation for Medical Research, NIH (1R01 AG033053, 1DP2 OD004345, and 5U01 HL100402), and Harvard Stem Cell Institute to A.J.W. Additional data are in the Supplement. J.C. was funded by NIH R01NS070835 and R01NS072167. L.L.R., A.J.W., R.T.L., and L.K. are inventors on a U.S. patent application filed by Harvard University and Brigham and Women's Hospital entitled "Methods and Compositions for Increasing Neurogenesis and Angiogenesis" (61/833,813).

Supplementary Materials

www.sciencemag.org/content/344/6184/630/suppl/DC1
Materials and Methods
Figs. S1 to S12
References (*33*–*34*)

22 January 2014; accepted 10 April 2014
10.1126/science.1251141

Identification of LRRC8 Heteromers as an Essential Component of the Volume-Regulated Anion Channel VRAC

Felizia K. Voss,[1,2,3] Florian Ullrich,[1,2,3] Jonas Münch,[1,2,3] Katina Lazarow,[1] Darius Lutter,[1,2,3] Nancy Mah,[2] Miguel A. Andrade-Navarro,[2] Jens P. von Kries,[1] Tobias Stauber,[1,2]* Thomas J. Jentsch[1,2,4]*

Regulation of cell volume is critical for many cellular and organismal functions, yet the molecular identity of a key player, the volume-regulated anion channel VRAC, has remained unknown. A genome-wide small interfering RNA screen in mammalian cells identified LRRC8A as a VRAC component. LRRC8A formed heteromers with other LRRC8 multispan membrane proteins. Genomic disruption of *LRRC8A* ablated VRAC currents. Cells with disruption of all five *LRRC8* genes required LRRC8A cotransfection with other LRRC8 isoforms to reconstitute VRAC currents. The isoform combination determined VRAC inactivation kinetics. Taurine flux and regulatory volume decrease also depended on LRRC8 proteins. Our work shows that VRAC defines a class of anion channels, suggests that VRAC is identical to the volume-sensitive organic osmolyte/anion channel VSOAC, and explains the heterogeneity of native VRAC currents.

Cells regulate their volume to counteract swelling or shrinkage caused by osmotic challenges and during processes such as cell growth, division, and migration. As water transport across cellular membranes is driven by osmotic gradients, cell volume regulation requires appropriate changes of intracellular concentrations of ions or organic osmolytes such as taurine (*1*, *2*). Regulatory volume decrease (RVD) follows the extrusion of intracellular Cl^- and K^+ and other osmolytes across the plasma membrane. A key player is the volume-regulated anion channel VRAC that mediates characteristic swelling-activated Cl^- currents [$I_{Cl(swell)}$] and is ubiquitously expressed in vertebrate cells (*3*–*5*). Nearly inactive under resting conditions, VRAC slowly opens upon hypotonic swelling. The mechanism behind VRAC opening remains enigmatic. VRAC currents are outwardly rectifying [hence the alternative name VSOR for volume-stimulated outward rectifier (*4*, *5*)] and show variable inactivation at inside-positive voltages. VRAC conducts iodide (I^-) better than chloride (Cl^-) and might also conduct organic osmolytes such as taurine (*6*) [hence VSOAC, volume-stimulated organic osmolyte/anion channel (*7*)], but this notion is controversial (*8*–*10*). VRAC is believed to be important for cell volume regulation and swelling-induced exocytosis (*11*) and also for cell cycle regulation, proliferation, and migration (*1*, *3*, *4*). It may play a role in apoptosis and various pathological states, including ischemic brain edema and cancer (*4*, *12*). Progress in the characterization of VRAC and its biological roles has been limited by the failure to identify the underlying protein(s) despite decades of efforts (*1*, *5*). ClC-2 Cl^- channels activate upon cell swelling, but their inward rectification and Cl^- over I^- selectivity deviate from VRAC (*13*). *Drosophila* dBest1, a member of a family of Ca^{2+}-activated Cl^- channels, mediates swelling-activated Cl^- currents in insect cells (*14*, *15*), but their characteristics differ from those of VRAC currents, and the mammalian homolog of dBest1 is swelling-insensitive (*16*). We show that VRAC represents a distinct class of anion channels that also conduct organic osmolytes.

To identify VRAC, we used a genome-wide RNA interference screen that could identify nonredundant VRAC components. Swelling-induced I^- influx into human embryonic kidney (HEK) cells expressing the I^--sensitive yellow fluorescent protein YFP(H148Q/I152L) (*17*) was used as readout in a fluorometric imaging plate reader (Fig. 1A). Exposure to saline containing 50 mM I^- yielded a slow fluorescence decay under isotonic conditions, whereas hypotonicity induced a delayed increase in YFP quenching (Fig. 1B) that could be reduced by VRAC inhibitors such as carbenoxolone (*18*) (fig. S1). In a prescreen targeting 21 anion transporters (table S1), only small interfering RNAs (siRNAs) against the Cl^-/HCO_3^- exchanger AE2 gave significant effects (Fig. 1B). They decreased I^- influx under both isotonic and hypotonic conditions.

Our genome-wide screen used three separately transfected siRNAs per gene (fig. S2). Offline data analysis (fig. S3, A and B) yielded the maximal slope of fluorescence quenching that was used to define hits. Further criteria included the presence of predicted transmembrane domains and a wide expression pattern. Eighty-seven genes (table S2) were taken into a secondary screen with independent siRNAs. Of these, only sup-

[1]Leibniz-Institut für Molekulare Pharmakologie (FMP), Berlin. [2]Max-Delbrück-Centrum für Molekulare Medizin (MDC), Berlin. [3]Graduate Program of the Freie Universität Berlin. [4]Neurocure, Charité Universitätsmedizin, Berlin.

*Corresponding author. E-mail: jentsch@fmp-berlin.de (T.J.J.); tstauber@fmp-berlin.de (T.S.)

Science

Vascular and Neurogenic Rejuvenation of the Aging Mouse Brain by Young Systemic Factors

Lida Katsimpardi, Nadia K. Litterman, Pamela A. Schein, Christine M. Miller, Francesco S. Loffredo, Gregory R. Wojtkiewicz, John W. Chen, Richard T. Lee, Amy J. Wagers and Lee L. Rubin

Science **344** (6184), 630-634.
DOI: 10.1126/science.1251141originally published online May 5, 2014

Help the Aged

Muscle function declines with age, as does neurogenesis in certain brain regions. Two teams analyzed the effects of heterochronic parabiosis in mice. **Sinha *et al.*** (p. 649) found that when an aged mouse shares a circulatory system with a youthful mouse, the aged mouse sees improved muscle function, and **Katsimpardi *et al.*** (p. 630) observed increased generation of olfactory neurons. In both cases, Growth Differentiation Factor 11 appeared to be one of the key components of the young blood.